Automotive Science and Engineering, Vol. 16, No. 3, (2026), 5107-5117

Iran University of Science and Technology

Automotive Science and Engineering

Journal Homepage: ase.iust.ac.ir

ISSN: 2008-9899

Investigation of the behavior of trapezoidal sandwich panels under high-velocity impact loading

M. Pahlavan[1], J. Marzbanrad[1]*

[1]School of Automotive Engineering, Vehicle Dynamic Systems Laboratory, Iran University of Science and Technology, 16846-13114, Tehran, Iran.

ARTICLE INFO

Article history:

Received : 3 Feb 2026

Accepted: 20 Jun 2026

Published: 13 Jul 2026

Keywords:

Energy absorption

High-velocity impact

Finite element

Honeycomb core

Trapezoidal sandwich panel

ABSTRACT

A trapezoidal sandwich panel with a mild steel honeycomb core was modeled under high-velocity impact loading generated by high-energy materials. Numerical simulations were performed at three impact energy levels for five sandwich panel configurations and an equivalent square plate of the same mass, for use in certain special vehicles. The deformation response of the sandwich panels and the equivalent square plate was comparatively evaluated. The results showed that the equivalent square plate exhibits the lowest specific energy absorption and the highest peak transmitted load among all the tested configurations. Panel P3, with approximately 145% higher energy absorption and about 66% lower peak transmitted force compared with the equivalent square plate, was identified as the most efficient design for impact energy dissipation. Therefore, this panel can be proposed as a cost-effective and efficient energy absorber for protecting equipment and occupants in various industrial applications.

1. Introduction

Energy-absorbing systems and multilayer structures play a critical role in the aerospace, automotive, and marine engineering industries, where they protect personnel and equipment from sudden impact loads [1]. Among various configurations, sandwich structures with honeycomb cores are widely used for their superior energy-dissipation characteristics. The impact response of these structures strongly depends on geometric parameters—including cell geometry, wall thickness, and flexural behavior of the structure [2-4]. as well as the overall material properties and the thickness of the core and face sheets [5-8]. Integrating honeycomb structures with graded configurations or multilayer architectures enhances the impact resistance of energy absorbers [9, 10].

Yang et al. investigated the crashworthiness of nested structures by assessing a system composed of a circular tube inserted inside an elliptical tube under compressive loading. Experimental and numerical analyses demonstrated that this nested configuration exhibits superior energy absorption performance compared with single circular or elliptical tubes, owing to its higher load-bearing stability under the applied loads [11].

Sandwich structures, due to their lightweight nature and adequate stiffness, are frequently employed for energy absorption and shock-wave resistance [12]. They have been used in circular tubular forms [13] and other geometric configurations [14]. In these structures, researchers have extensively optimized energy absorption [15, 16], commonly by modifying wall thickness, altering the core material, and adjusting geometric dimensions [17]. These panels are typically filled

*Corresponding Author
Email Address: marzban@iust.ac.ir
https://doi.org/10.22068/ase.2026.755

with materials such as aluminum foam [18], reinforced composites [19, 20], or polymer blends containing carbon nanotubes [21] to improve their impact resistance.

Pahlavan and Marzbanrad examined the behavior of a trapezoidal sandwich panel with a polyurethane foam core under low-velocity impact using both numerical and experimental approaches. Their findings indicated that the hybrid panel exhibits superior performance and higher energy absorption capacity than its individual components [22]. Zhang et al. subjected CFRP honeycomb sandwich structures to high-velocity impact and analyzed the energy absorption and damage mechanisms experimentally and numerically. Their study revealed that face sheet deformation occurs before complete failure, and that core instability (buckling) evolves into crushing and shear failure. Furthermore, the findings indicated that the dominant energy absorption mechanisms arise primarily from fiber fracture and interlaminar delamination rather than stable, progressive core deformation [23]. Slawinski et al. aimed to mitigate shock-wave-induced loads in vehicles and numerically simulated multilayer energy-absorbing panels composed of low-density materials with varying stiffnesses using LS-DYNA. They evaluated the structural response under two shock-wave scenarios: underbody and lateral loading. The effectiveness of the panels in attenuating energy was assessed by analyzing the acceleration-time histories recorded at selected locations on the vehicle body [24]. To enhance the protective level of vehicle floors against shock waves, Abdelwahab et al. employed a composite configuration reinforced with aluminum foam. The researchers validated the accuracy of their numerical model by conducting experimental tests and comparing them with the numerical predictions. Analysis of displacement–time parameters for these sandwich panels demonstrated that using aluminum foam as reinforcement significantly improves structural resistance and performance under shock-wave loading [25]. Starczewski et al. experimentally investigated the performance of multi-material spaced panels equipped with energy absorbers to simulate an underbody shock-wave event in vehicles. By mounting the protective system on a ballistic pendulum and applying a shock load generated by a spherical charge, the researchers accurately quantified the energy absorbed by the structure based on the pendulum swing amplitude [26]. Yadaki et al. evaluated the performance of a multilayer sandwich panel comprising special steel and aluminum, aluminum foam, and glass-fiber composite against underbody shock waves in vehicles. According to the relevant standard, they tested the structure against a level 3 threat. The investigations showed good agreement between numerical simulations and experimental data, and the results confirmed the high energy-absorption capability of these panels [27].

Recent studies on energy-absorbing structures subjected to high-velocity impact have shown that high-strength materials are predominantly used as front face sheets, and that energy absorption in these configurations mainly occurs through damage, failure, and perforation of the protective panels safeguarding equipment and occupants. At the same time, stable buckling and progressive crushing have received comparatively less attention. Moreover, given the high cost of experimental impact testing, a common and rapid approach to evaluating energy absorbers under high-velocity impact is to use numerical simulations under the corresponding loading conditions.

Accordingly, this study used numerical simulation to assess the performance of a sandwich panel and an equivalent solid plate under high-velocity impact. In this context, a medium-strength steel was employed, and a honeycomb core confined within a trapezoidal sandwich panel was used to enhance the absorber's energy-absorption capacity. The study investigated the influence of the panel structural configuration, compared with an equal-weight solid plate, and the effect of thickness variation on absorbed energy, transmitted load to the occupant, and deflection of the panel's top and bottom plates.

2. Numerical Analysis

The high-velocity numerical analysis modeled the sandwich panels and the equivalent square plate under impact loading corresponding to different shock-wave energy levels generated by high-energy materials. The equivalent square plate, along with the top and bottom face sheets and the honeycomb core, was modeled using four-node shell elements (S4R).

2.1. Modeling of the Equivalent Square Plate

The equivalent square plate, with dimensions of 300 x 300 x 5 mm and made of mild steel, was designed to have a mass approximately equal to that of the sandwich panels P1-P4 (Table 3) and was subjected to shock loading generated by high-energy materials with charges of 50, 150, and 250 g. The modeling used the CONWEP method, as illustrated in Fig. 1, where the high-energy material

[DOI: 10.22068/ase.2026.755]

is located 100 mm from the center of the equivalent square plate. To represent the strain-rate-dependent plastic response of the equivalent square plate under shock-wave loading, the Johnson–Cook constitutive model was employed. The equivalent von Mises yield stress is expressed as:

$$\sigma_y = (A + B(\bar{\varepsilon}^p)^n)\left[1 + C\ln\left(\frac{\dot{\bar{\varepsilon}}^p}{\dot{\varepsilon}_0}\right)\right] * [1 - (T^*)^m] \quad (2)$$

where A is the Yield stress constant, B and n are Strain hardening constant, C is the Viscous effect, and mis the thermal softening constant. In this equation, $\bar{\varepsilon}^p$and $\dot{\bar{\varepsilon}}^p$ denote the equivalent plastic strain and equivalent plastic strain rate, respectively. The reference plastic strain rate is represented by $\dot{\varepsilon}_0$, and the normalized temperature is defined as:

$$T^* = \frac{T - T_r}{T_m - T_r}$$

where Tis the current material temperature, T_r is the reference temperature, and T_m is the melting temperature of the material. The Johnson–Cook parameters adopted for the mild steel, together with its principal elastic and physical properties [28], are listed in Table 1. The Johnson–Cook damage and failure formulation was not activated in the present simulations. Within the investigated loading range, the predicted response was governed primarily by global plastic deformation, bending, local buckling, and progressive folding, without evidence of material fracture, separation, or perforation. Therefore, the constitutive model was used to describe the plastic flow and strain-rate effects, while the damage and failure response was outside the scope of the present analysis. Fully clamped boundary conditions were imposed, and, based on mesh sensitivity analysis, a mesh size of 10 mm was selected. To improve through-thickness accuracy, nine integration points were specified through the thickness of the plate. For comparison of the output quantities of the equivalent square plate with those of the sandwich panels, the deflection from the center to the edge of the equivalent square plate under shock-wave loading with 50, 150, and 250 g of energetic material was plotted in Fig. 2. To validate the numerical model, the numerical procedure was assessed by comparing the results with the experimental data reported by Dharmasena et al. [29]. The geometry, material properties, boundary conditions, and shock-wave loading conditions of the reference plate were reproduced in Abaqus/Explicit using the CONWEP formulation.

Table 2 presents a quantitative comparison between the experimental measurements, the numerical results reported in the reference study, and the current finite-element predictions. We determined the relative error (e) for each case using Equation (1).

$$e(\%) = \frac{|D_{FE} - D_{Exp}|}{D_{Exp}} \times 100 \quad (1)$$

Where D_{FE} and D_{Exp} denote the numerical and experimental center displacement values, respectively. The comparison confirms that the adopted finite-element procedure reproduces the reference steel plate's shock-wave response with acceptable accuracy across the investigated load levels. This validation applies to the shock-wave loading and structural-modeling methodology. Because the proposed trapezoidal sandwich–honeycomb architecture is a newly designed configuration with no identical experimental specimen in the literature, the sandwich-panel results are presented as numerical predictions. Future experimental assessment of this specific architecture is recommended.

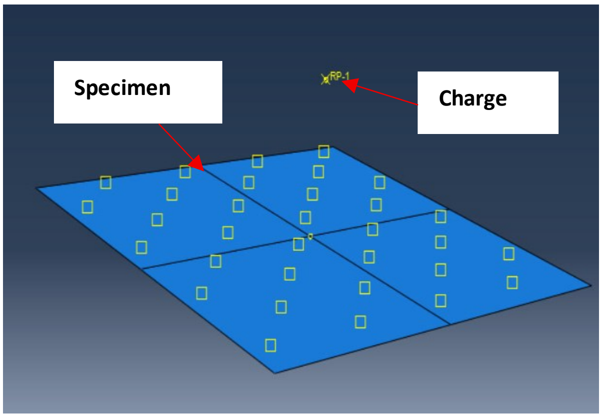

Figure 1. Finite element model for an equivalent square sheet under high-velocity impact test

Table 1: Johnson-Cook coefficients and material properties of mild steel

A (MPa)	B (MPa)	C	n	m	T_m (K)
304	422	0.0156	0.345	0.87	1800

Table 1: (Continued)

$\dot{\varepsilon}_0(\mathrm{s}^{-1})$	T_r(K)	ρ(kg m^{-3})	E(GPa)	ν
0.0001	293	7850	210	0.32

[DOI: 10.22068/ase.2026.755]

Table 2: Comparison of experimental and numerical deflections of the equivalent plate

High-energy material (kg)	Exp. center deflection (mm) [29]	Num. center deflection (mm) [29]	Present Num. center deflection (mm)	Error of Num. (%) [29]	Error of Present Num. (%)
1	37.65	47.22	48.54	25.4	28.9
2	71.37	80.93	88.38	13.4	23.8
3	132.94	108.9	109.75	18.1	17.4

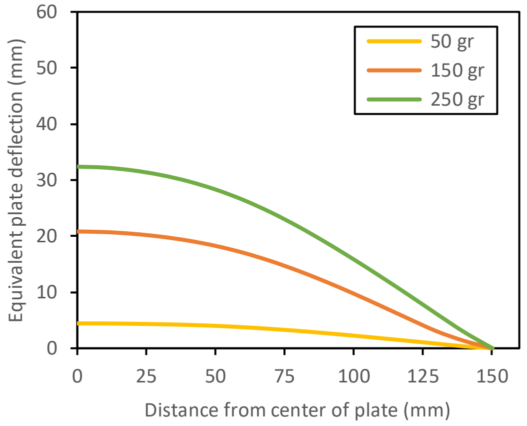

Figure 2. Equivalent plate deflection under different impact energy levels

2.2. Modeling of the Sandwich Panel

Four types of metallic sandwich panels with overall dimensions of 300×300×64 mm, each consisting of a trapezoidal metal framework and a honeycomb core confined within the panel, were selected for numerical modeling. All components were made of mild steel. The geometric configuration of the investigated panels is schematically illustrated in Fig. 3. The internal core architecture consists of trapezoidal webs filled with regular hexagonal honeycomb elements having a side length of 35 mm, a horizontal pitch of 70 mm, and an internal apex angle of 120°. The thicknesses of the face-sheets and the core walls are designated by t_f and t_c, respectively, and their assigned values for the four panel configurations (P1–P4) are listed in Table 2. The boundary conditions were defined by fully constraining the peripheral edges of the panels. To simulate the shock-wave loading using the CONWEP approach, the charge was positioned at a distance of 100 mm from the center of the top face sheet of the sandwich panel, as illustrated in Fig. 4. The charge mass was selected as 50, 150, and 250 g to generate three distinct loading intensity levels. To improve computational accuracy, A mesh sensitivity analysis was conducted, as illustrated in Fig. 5, by systematically varying the element size from 16 mm to 6 mm. As the mesh size decreased, the maximum stress gradually converged; the change between the 10 mm and 8 mm meshes was limited to about 3%, indicating that the modeling results are essentially mesh-independent. Consequently, an optimal shell element size of 10 mm was adopted, providing a suitable balance between result accuracy and computational time. An automatic surface-to-surface contact algorithm was defined to model the interaction between the face sheets and the honeycomb core. The Interaction module established the coupling between the shock wave and the panel's top face sheet by defining a reference point and an impact surface using the Air Blast option. The reference point, defined through the Interaction Property, was used to specify the charge mass so that the shock wave impact is directly transmitted to the top surface of the panel. To account for strain-rate effects in the high-velocity impact response, the Johnson–Cook constitutive model was employed, using the mechanical data for mild steel listed in Table 1. Figs. 6 and 7 present the deformation patterns at various panel locations and the final deflection from the center to the edge of the top face sheets under impact energy levels corresponding to 50, 150, and 250 gr of high-energy material, respectively.

Table 3: Honeycomb sandwich panels and equivalent square plate geometry

Panel	Sheet thickness t_f (mm)	Honeycomb thickness t_c (mm)	Weight (kg)
P1	1	1.25	3.6
P2	1.25	0.9	3.51
P3	1.5	0.6	3.50
P4	1.75	0.3	3.49
Equ. Plate	5	-	3.53

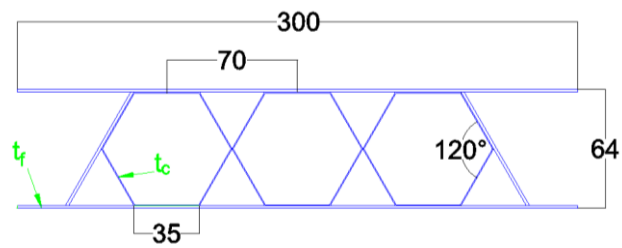

Figure 3. Cross-sectional geometry and dimensions of the sandwich panel (dimensions in mm).

[DOI: 10.22068/ase.2026.755]

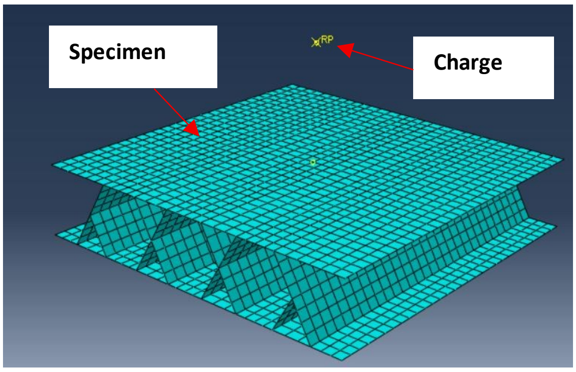

Figure 4. Finite element model for sandwich panel under high-velocity impact test

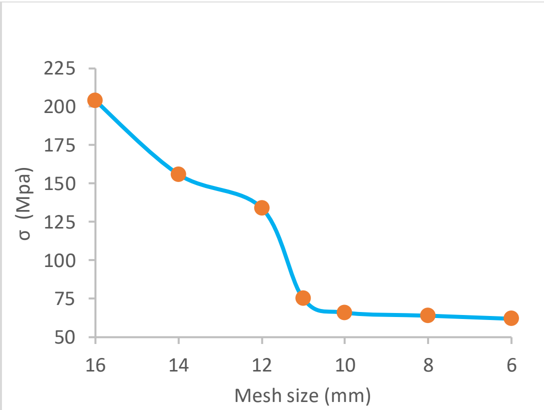

Figure 5. Mesh sensitivity and stress convergence curve

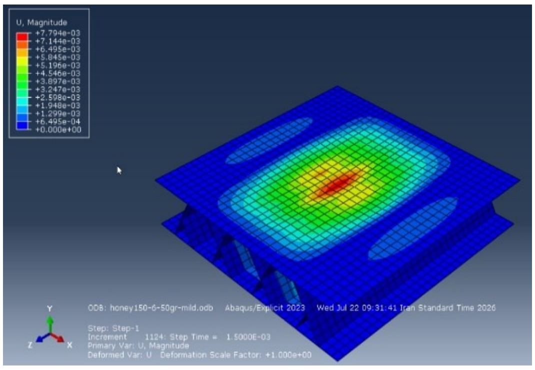

(a)

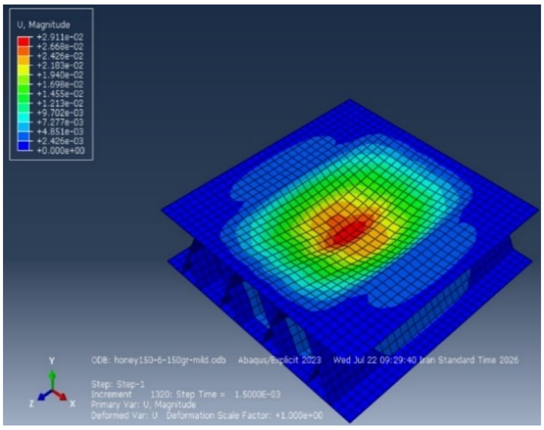

(b)

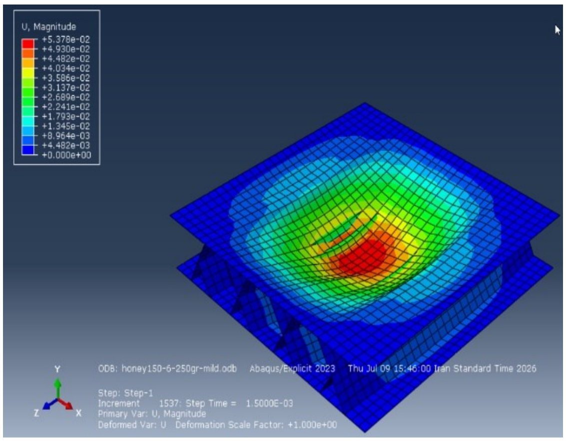

(c)

Figure 6. Sandwich panel deflection under different impact energy levels: (a) 50gr High-energy materials (b) 150gr High-energy materials (c) 250gr High-energy materials

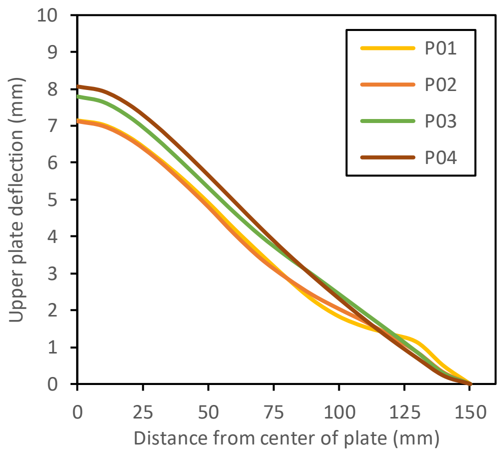

(a)

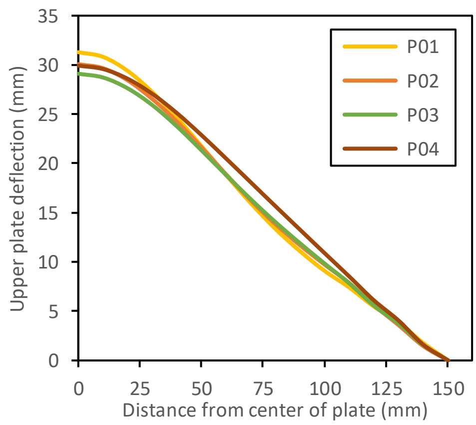

(b)

[DOI: 10.22068/ase.2026.755]

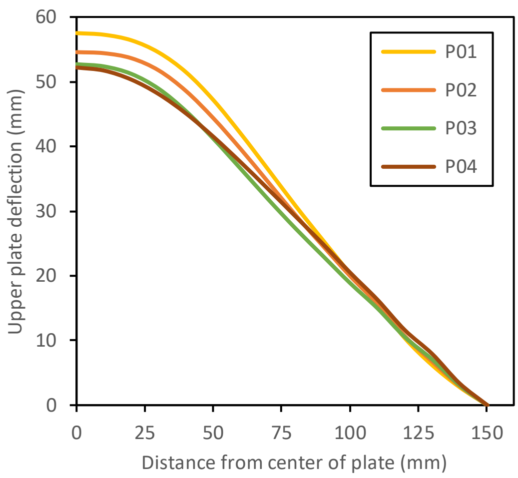

(c)

Figure 7. Sandwich panels upper plate deflection under different impact energy levels: (a) 50 gr High-energy materials (b) 150 gr High-energy materials (c) 250 gr High-energy materials

3. Results and Discussion

3.1. Interaction Mechanism of Components and the Effect of Thickness Variation on Panel Deformation

Under shock-wave loading, panels P1–P4 were subjected to different loading intensities generated by explosive masses ranging from 50 to 250 g. The panel components, including the honeycomb core, front and rear face sheets, and surrounding side walls, interacted to resist the applied shock-wave load. Confinement of the honeycomb core within the trapezoidal framework constrained lateral deformation, modified the crushing process, and enhanced progressive energy absorption. The shock-wave energy was dissipated primarily through the combined plastic deformation of the front and rear face sheets and the progressive deformation of the honeycomb core. The main deformation mechanisms included local indentation of the loaded front face sheet, plastic bending and stretching of the face sheets, buckling and progressive folding of the honeycomb cell walls, and mechanical interaction between the deformed cell walls and the surrounding trapezoidal framework. As the front face sheet was subjected to the incident shock wave, local indentation developed in the impact region and was followed by bending and in-plane plastic stretching of the face sheet. The resulting deformation was transferred to the honeycomb core, where the cell walls underwent buckling and progressive folding. The rear face sheet subsequently participated in the global deformation response and provided additional resistance against core collapse and panel deflection. These coupled deformation mechanisms increased the effective plastic deformation path and distributed the shock-wave load over a larger portion of the panel. Consequently, the load transmitted to the rear face sheet and the supported boundaries was reduced compared with a response dominated by localized deformation of the front face sheet alone. The thickness of the face sheets and the honeycomb-core walls affected the relative contribution of these mechanisms by modifying the bending stiffness, axial resistance, local buckling capacity, and crushing resistance of the panel components. Therefore, variations in thickness changed the deformation pattern and the balance between face-sheet bending, core crushing, cell-wall folding, and interaction with the surrounding trapezoidal framework.

According to the results presented in Fig. 8, for all panels impacted by the energetic material, increasing the charge mass from 50 to 250 g leads to a nonlinear increase in the deformation of the top and bottom face sheets. The bottom sheet deflection gradually increases from the plate edge toward the center, reaching its maximum at the plate center. As shown in Fig. 9, a comparison between panels P1–P4 and the equivalent square plate indicates that increasing the thickness of the top, bottom, and side sheets of the trapezoidal panel enhances its stiffness and reduces the central deflection of the top and bottom sheets. From Fig. 10, it is observed that the center-to-edge deformation of the bottom sheets of all panels, at all impact energy levels corresponding to 50–250 g of energetic material, is lower than that of the equivalent square plate. This finding confirms that a significant portion of the impact energy is absorbed within the sandwich panel and is not transmitted to the bottom sheet, thereby reducing the magnitude of the impact load transferred.

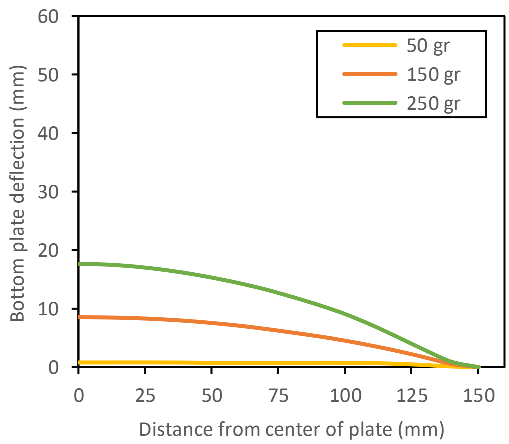

(a)

[DOI: 10.22068/ase.2026.755]

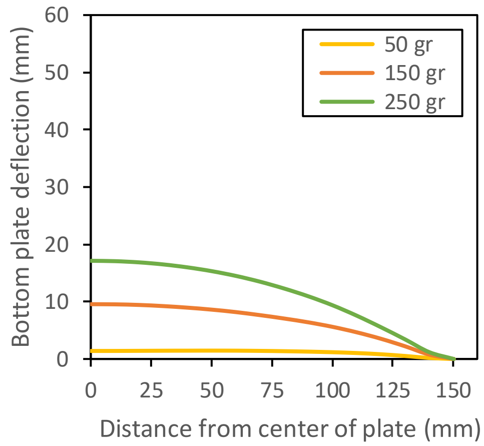

(b)

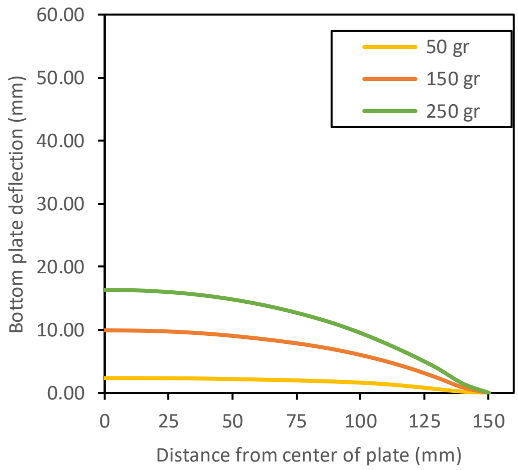

(c)

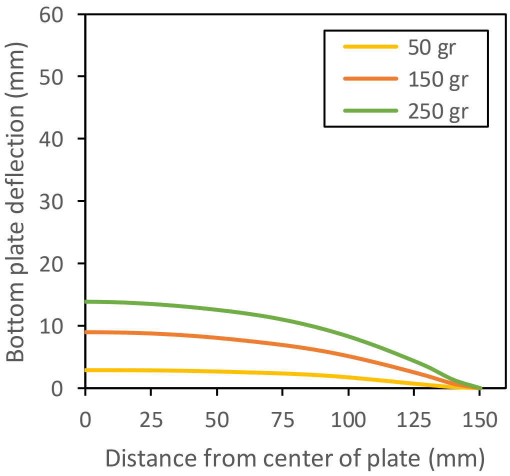

(d)

Figure 8. Sandwich panel bottom plate deflection under different impact energy levels: (a) P1, (b) P2, (c) P3, (d) P4

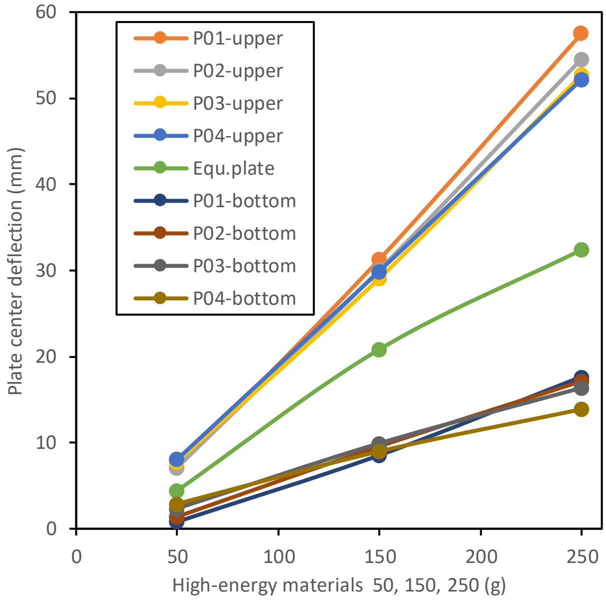

Figure 9. Comparison of the sandwich panels and equivalent plate deflection under different impact energy levels

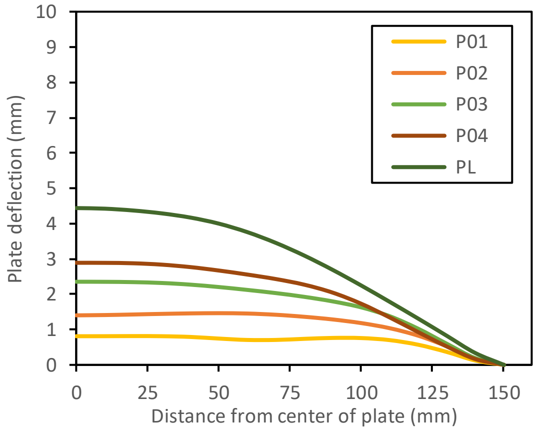

(a)

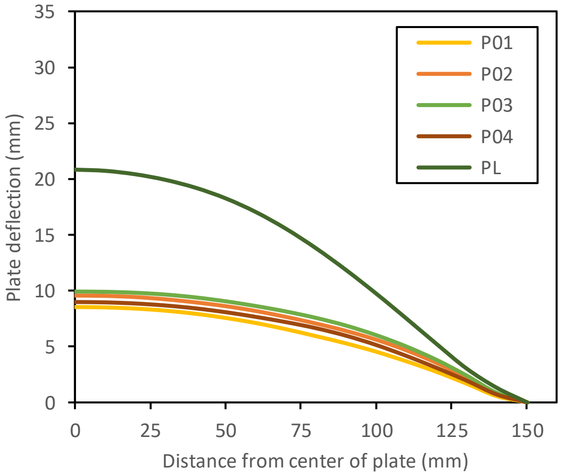

(b)

[DOI: 10.22068/ase.2026.755]

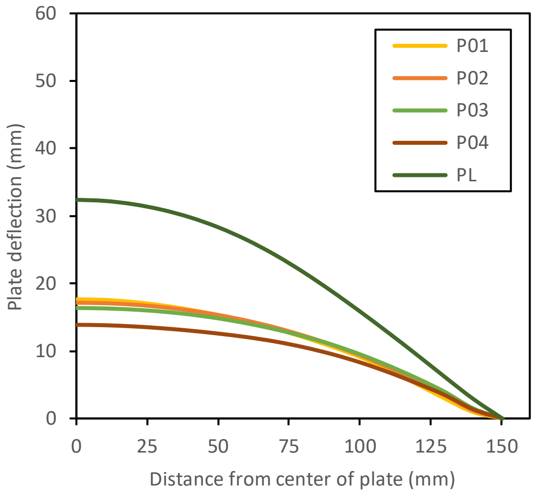

(c)

Figure 10. Comparison of sandwich panel bottom plate and equivalent plate deflection under different impact energy levels: (a) 50gr High-energy materials, (b) 150gr High-energy materials, (c) 250gr High-energy materials

3.2. Effect of Thickness Variation on Specific Energy Absorption and Maximum Transmitted Load

In industries such as automotive, aerospace, and marine engineering, lightweight yet impact-resistant structures are essential. Accordingly, specific energy absorption is a key criterion for selecting a suitable energy absorber for these applications.

In the present numerical study, the energy dissipated through plastic deformation was obtained from the Abaqus/Explicit history output variable E_{PD}. The E_{PD} variable represents the total energy dissipated by plastic deformation in the modeled structure. Therefore, it was used as the numerical measure of the energy absorbed (EA) by each panel. This energy was mainly dissipated through plastic deformation of the front and rear face sheets, progressive buckling and folding of the honeycomb cell walls, and deformation of the surrounding trapezoidal framework, as described in Section 3.1. The specific energy absorption was calculated by normalizing the plastic energy dissipation with respect to the total mass of the corresponding structure by using Equation (3).

$$SEA = \frac{EA\ (J)}{m\ (kg)} \tag{3}$$

where m is the total mass of the corresponding panel or equivalent square plate. The SEA value is reported in J/kg. Since the total mass of the sandwich panels was maintained within a narrow range, this normalization enabled a meaningful comparison of their mass-specific energy absorption performance.

In the selected panels (P1 to P4), the thickness of the main sheets of the trapezoidal panel increases gradually, while the core sheet thickness decreases to keep the panel weight constant. The amount of absorbed energy differs among the panels, mainly because the average load applied to each panel varies. To evaluate the effect of changes in panel sheet thickness on specific energy absorption, the bar chart of specific energy absorption for all panels and the equivalent square plate under shock-wave loading generated by 250 g of energetic material is presented in Fig. 11. Comparison of the specific energy absorption of the five panel types with that of the equivalent plate shows, firstly, that employing the trapezoidal panel with a honeycomb core of various thickness configurations consistently provides better impact energy absorption than the equivalent square plate. This improvement is attributed to the coordinated plastic deformation of the face sheets, progressive buckling and folding of the honeycomb cell walls, and deformation of the surrounding trapezoidal framework. These mechanisms provide a larger plastic deformation path and promote the dissipation of a greater amount of energy per unit mass. Second, panel P3, with a main sheet thickness of 1.5 mm and a core sheet thickness of 0.6 mm, exhibits the highest specific energy absorption. In contrast, the equivalent square plate with a thickness of 5 mm shows the lowest energy absorption. The specific energy absorption of panel P3 is approximately 145% higher than that of the equivalent square plate. To assess the effect of thickness variation on the maximum transmitted load, the peak force diagram for all panels P1 to P4 and the equivalent square plate under shock-wave loading generated by 250 g of high-energy material is plotted in Fig. 12. Comparison of the values indicates that the maximum force transmitted through all sandwich panels is lower than that of the equivalent square plate. This implies that replacing the equivalent square plate with the trapezoidal sandwich panel enhances energy absorption and reduces load transfer to the equipment and/or occupants. Among the panels, P1 exhibits the highest peak load. This value gradually decreases from panel P1 to P3 as the core sheet thickness decreases and the thickness of the

[DOI: 10.22068/ase.2026.755]

trapezoidal panel sheets increases. From panel P4 onwards, the peak load starts to increase again. This is because, initially, reducing the core thickness decreases panel resistance; however, with further reduction, the honeycomb core's contribution diminishes, and the overall panel resistance is dominated by the increased thickness of the trapezoidal sheets, leading to a higher maximum transmitted load. In the optimum configuration, the peak load for panel P3 was 192 kN, which represented a reduction of about 66% compared with the equivalent square plate.

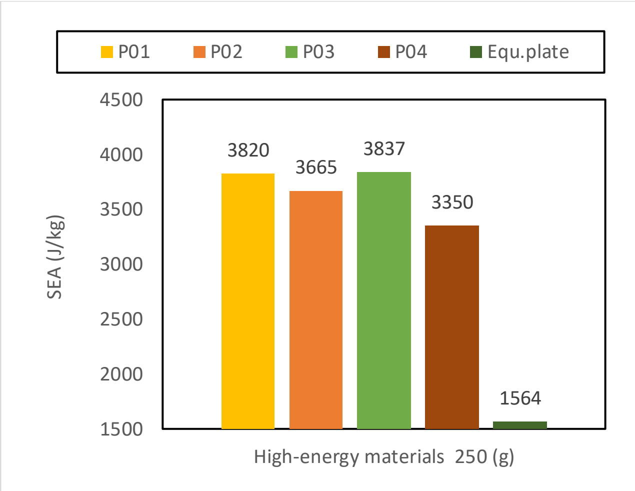

Figure 11. Specific energy absorption of sandwich panels and equivalent plate under 250gr High-energy materials impact energy level

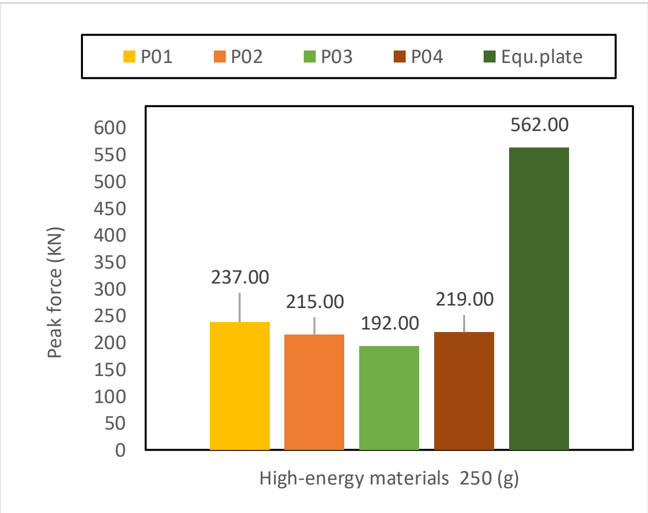

Figure 12. Peak force of sandwich panels and equivalent plate under 250 gr High-energy materials impact energy level

4. Conclusion

In this study, a trapezoidal sandwich panel with a honeycomb core and a square plate with an equivalent mass were subjected to high-velocity impact. The results showed that, across all configurations with different thicknesses of the top, bottom, and core sheets, the sandwich panel consistently exhibits higher specific energy absorption and lower peak transmitted load than the equivalent square plate.

Furthermore, examining peak load across the panels showed that the maximum force decreases from P1 to P3 as core thickness decreases, whereas from P3 to P4, due to the increased thickness of the trapezoidal panel sheets, the effect of reduced core thickness diminishes and the peak load rises again. In the optimal configuration (panel P3), the specific energy absorption was approximately 145% higher than that of the equivalent square plate, whereas the maximum transmitted force was approximately 66% lower. In addition, using mild steel sheets instead of high-strength steel in these panels lowers the material and manufacturing costs.

Therefore, panel P3 is the most efficient configuration in terms of specific energy absorption and peak transmitted load reduction, making it a suitable candidate for use as an energy absorber in various industries to protect equipment and occupants against high-velocity impacts.

Declaration of Conflicting Interests

The author(s) declared no potential conflicts of interest with respect to the research, authorship, and/or publication of this article.

List of symbols

E	Modulus of elasticity
SEA	Specific Energy Absorption
ρ	Density
ν	Poisson's ratio

Greek symbols

σ	Von Mises stress

[DOI: 10.22068/ase.2026.755]

References

[1] B. Bakri and M. Fadly, "Investigation on ballistic impact properties of rattan fiber-reinforced high-density polyethylene composite material," *International Journal of Engineering,* vol. 39, pp. 870-879, 2026.

[2] D. Muniraj and V. Sreehari, "Experimental damage evaluation of honeycomb sandwich with composite face sheets under impact load," 2021.

[3] F. N. Habib, P. Iovenitti, S. H. Masood, and M. Nikzad, "Cell geometry effect on in-plane energy absorption of periodic honeycomb structures," *The International Journal of Advanced Manufacturing Technology,* vol. 94, no. 5, pp. 2369-2380, 2018/02/01 2018, doi: 10.1007/s00170-017-1037-z.

[4] W. He, L. Yao, X. Meng, G. Sun, D. Xie, and J. Liu, "Effect of structural parameters on low-velocity impact behavior of aluminum honeycomb sandwich structures with CFRP face sheets," *Thin-Walled Structures,* vol. 137, pp. 411-432, 2019/04/01/ 2019.

[5] G. Sun, X. Huo, H. Wang, P. J. Hazell, and Q. Li, "On the structural parameters of honeycomb-core sandwich panels against low-velocity impact," *Composites Part B: Engineering,* vol. 216, p. 108881, 2021/07/01/ 2021.

[6] V. Birman and G. A. Kardomateas, "Review of current trends in research and applications of sandwich structures," *Composites Part B: Engineering,* vol. 142, pp. 221-240, 2018/06/01/ 2018.

[7] T. Thomas and G. Tiwari, "Crushing behavior of honeycomb structure: a review," *International Journal of Crashworthiness,* vol. 24, no. 5, pp. 555-579, 2019/09/03 2019, doi: 10.1080/13588265.2018.1480471.

[8] X. Zhang, F. Xu, Y. Zang, and W. Feng, "Experimental and numerical investigation on damage behavior of honeycomb sandwich panel subjected to low-velocity impact," *Composite Structures,* vol. 236, p. 111882, 2020/03/15/ 2020.

[9] S. R. G. Bates, I. R. Farrow, and R. S. Trask, "Compressive behaviour of 3D printed thermoplastic polyurethane honeycombs with graded densities," *Materials & Design,* vol. 162, pp. 130-142, 2019/01/15/ 2019

[10] O. A. Ganilova and J. J. Low, "Application of smart honeycomb structures for automotive passive safety," *Proceedings of the Institution of Mechanical Engineers, Part D: Journal of Automobile Engineering,* vol. 232, no. 6, pp. 797-811, 2018, doi: 10.1177/0954407017708916.

[11] X. Yang, J. Ma, Y. Sun, and J. Yang, "An internally nested circular-elliptical tube system for energy absorption," *Thin-Walled Structures,* vol. 139, pp. 281-293, 2019/06/01/ 2019.

[12] P. Tran, S. Linforth, T. D. Ngo, R. Lumantarna, and T. Q. Nguyen, "Design analysis of hybrid composite anti-ram bollard subjected to impulsive loadings," *Composite Structures,* vol. 189, pp. 598-613, 2018.

[13] N. Jones, *Structural impact*. Cambridge University Press, 2011.

[14] A. Alghamdi, "Collapsible impact energy absorbers: an overview," *Thin-walled structures,* vol. 39, no. 2, pp. 189-213, 2001.

[15] Z. Wang, Y. Zhou, X. Wang, and X. Zhang, "Multi-objective optimization design of a multi-layer honeycomb sandwich structure under blast loading," *Proceedings of the Institution of Mechanical Engineers, Part D: Journal of Automobile Engineering,* vol. 231, no. 10, pp. 1449-1458, 2017.

[16] S. Nayak, A. K. Singh, A. Belegundu, and C. Yen, "Process for design optimization of honeycomb core sandwich panels for blast load mitigation," *Structural and Multidisciplinary Optimization,* vol. 47, no. 5, pp. 749-763, 2013.

[17] S. C. K. Yuen, G. Cunliffe, and M. Du Plessis, "Blast response of cladding sandwich

panels with tubular cores," *International Journal of Impact Engineering,* vol. 110, pp. 266-278, 2017.

[18] M. Altenaiji, Z. W. Guan, W. Cantwell, and Y. Y. Zhao, "Characterisation of aluminium matrix syntactic foams dynamic loading," *Applied Mechanics and Materials,* vol. 564, pp. 449-454, 2014.

[19] S. Pichandi, S. Rana, D. Oliveira, and R. Fangueiro, "Fibrous and composite materials for blast protection of structural elements—A state-of-the-art review," *Journal of Reinforced Plastics and Composites,* vol. 32, no. 19, pp. 1477-1500, 2013.

[20] A. Christian and G. O. K. Chye, "Performance of fiber reinforced high-strength concrete with steel sandwich composite system as blast mitigation panel," *Procedia Engineering,* vol. 95, pp. 150-157, 2014.

[21] M. M. R. Taha, A. B. Colak-Altunc, and M. Al-Haik, "A multi-objective optimization approach for design of blast-resistant composite laminates using carbon nanotubes," *Composites Part B: Engineering,* vol. 40, no. 6, pp. 522-529, 2009.

[22] M. Pahlavan and J. Marzbanrad, "Energy absorption capacity of trapezoidal sandwich panels with polyurethane foam under low-velocity impact loading," *International Journal of Engineering,* vol. 40, no. 2, pp. 540-554, 2027, doi: 10.5829/ije.2027.40.02b.16.

[23] R. Zhanga, Y. Wanga, X. Weia, and J. Xionga, "Experimental and numerical study of high-velocity impact behavior of carbon fiber honeycomb sandwich structures," *International Journal of Impact Engineering,* 2025.

[24] G. Sławiński, P. Malesa, and M. Świerczewski, "Numerical assessment regarding the influence of the stiffness of the material used to build multi-layer energy-absorbing panels on the absorption of the shock wave energy," in *International Conference on Computational & Experimental Engineering and Sciences*, 2019: Springer, pp. 61-79.

[25] M. M. Abdel Wahab, S. Mazek, and M. M. Abada, "Effect of blast wave on lightweight structure performance," *Journal of Engineering Science and Military Technologies,* vol. 1, no. 1, pp. 1-6, 2017.

[26] L. Starczewski, K. Szcześniak, M. Gmitrzuk, and R. Nyc, "Determining the degree of pulse absorption of air blast wave by spaced material systems," *Materiały Wysokoenergetyczne,* vol. 12, 2020.

[27] R. Řídký, J. Buchar, S. Rolc, M. Drdlová, and J. Krátký, "Numerical explicit analysis of absorbing materials used in multilayer mine protection," *Engineering Mechanics,* 2014.

[28] M. A. Iqbal, K. Senthil, P. Bhargava, and N. K. Gupta, "The characterization and ballistic evaluation of mild steel," *International Journal of Impact Engineering,* vol. 78, pp. 98-113, 2015/04/01/ 2015.

[29] K. P. Dharmasena, H. N. G. Wadley, Z. Xue, and J. W. Hutchinson, "Mechanical response of metallic honeycomb sandwich panel structures to high-intensity dynamic loading," *International Journal of Impact Engineering,* vol. 35, no. 9, pp. 1063-1074, 2008/09/01/ 2008.

[DOI: 10.22068/ase.2026.755]